Correlations due to Localization in Quantum Eigenfunctions of Disordered Microwave Cavities

Prabhakar Pradhan and S. Sridhar

Department of Physics, Northeastern University, Boston, Massachusetts 02115

(Received 28 February 2000)

Statistical properties of experimental eigenfunctions of quantum chaotic and disordered microwave cavities are shown to demonstrate nonuniversal correlations due to localization. Varying energy E and mean free path l enable us to experimentally tune from localized to delocalized states. Large level-to-level inverse participation ratio (I_2) fluctuations are observed for the disordered billiards, whose distribution is strongly asymmetric about $\langle I_2 \rangle$. The spatial density autocorrelations of eigenfunctions are shown to spatially decay exponentially and the decay lengths are experimentally determined. All the results are quantitatively consistent with calculations based upon nonlinear sigma models.

PACS numbers: 73.23.–b, 05.45.Mt, 73.20.Dx, 73.20.Fz

The universal properties of quantum chaotic systems have been extensively studied in terms of their eigenvalue and eigenfunction statistics [1]. In random matrix theory (RMT), the Gaussian distribution of eigenfunction amplitudes $\psi(\vec{r})$ leads to the universal Porter-Thomas (PT) distribution for the densities $|\psi|^2$, which has been observed in microwave cavities [2] as well as other systems. However, nonuniversality has important manifestations, for instance, due to periodic orbits which lead to scars in eigenfunctions, and localization arising from quantum interference in diffusion. While there have been many theoretical treatments, from semiclassical periodic orbit theories [1] to nonlinear sigma models [3], there have been few experimental studies of eigenfunctions because of their lack of accessibility.

In this paper, we present several striking manifestations of localization in experimental eigenfunctions of disordered microwave billiard cavities. Localization due to boundary or impurity scattering results in correlations that affect statistics and spatial correlations of the eigenfunctions in several measures, leading to deviations from their universal values for quantum chaotic systems. The moments of the density distribution, $I_n = \int |\Psi(\vec{r})|^{2n} d^3r$, in particular, the inverse participation ratio I_2 (IPR), and their distributions $P_{I_n}(I_n)$, are important measures of the properties of the chaotic and disordered eigenfunctions. In chaotic billiards, I_2 has a mean value $\langle I_2 \rangle$ close to that of the universal two-dimensional 2D limiting value of 3.0, with small level-to-level fluctuations $\delta I_2 \ll \langle I_2 \rangle$, resulting in a nearly symmetric distribution about $\langle I_2 \rangle$. In disordered billiards not only is the mean value $\langle I_2 \rangle \gg 3.0$, but the fluctuations are also much greater $\delta I_2 \sim \langle I_2 \rangle$. The IPR distribution for the disordered billiards is strongly asymmetric about $\langle I_2 \rangle$, and is quantitatively consistent with the calculations based upon the nonlinear sigma models of supersymmetry, parametrized by a conductivity g [4,5]. Spatial correlations are studied in terms of the density autocorrelation $\langle |\Psi(r)|^2 |\Psi(r')|^2 \rangle$ and are shown to die out more rapidly in the disordered billiards compared with the chaotic geometries with a characteristic decay length given by the mean free path l. Here again the data are in quantitative agreement with the sigma model calculations. Our results represent the first quantitative comparison of experiments and theory.

The experiments were carried out using thin (height $d <$ 6 mm) cavities, whose cross sections can be shaped in essentially arbitrary geometries. For these two-dimensional cavities, the operational wave equation is $(\nabla^2 + k^2)\Psi = 0$, with Dirichlet boundary conditions $\psi = 0$ at metallic boundaries; $\psi = E_z$ is the microwave electric field. Similar microwave experiments, which exploit this quantum mechanical—electromagnetic (QM-EM) mapping, have been used to study quantum chaos in closed [6,7] and open systems [8]. Eigenfunctions $|\psi(r)|^2$ were directly measured using a cavity perturbation technique [6]. Localization effects were observed by fabricating billiards in which 1 cm circular tiles were placed in a 44 cm $\times$ 21.8 cm rectangle at random locations (Fig. 1) to act as hard scatterers. (The locations were generated using a random number generator and the tiles placed manually.) Several realizations

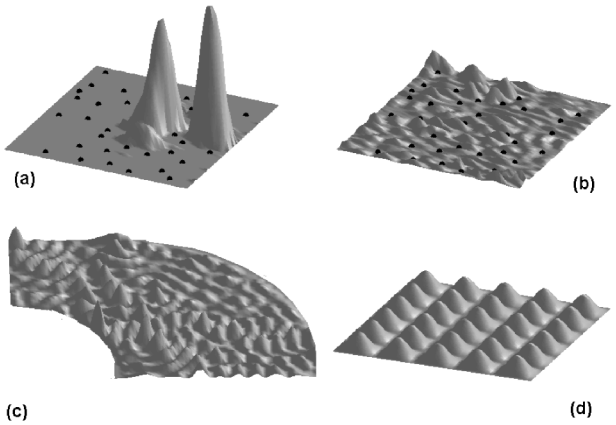

FIG. 1. (a),(b) Experimental eigenfunctions of a disordered billiard with $n = 36$ scatterers (noted by the black dots) (a) a strongly localized state, $f = 3.04$ GHz, $I_2 = 13.42$ and (b) a delocalized state $f = 7.33$ GHz, $I_2 = 4.06$. Eigenfunctions of (c) Sinai-stadium billiard $I_2 = 3.01$; (d) an integrable rectangle ($I_2 = 2.25$ for all states).

 0031-9007/00/85(11)/2360(4)$15.00

of the disordered geometry were experimentally studied, by varying the density of scatterers from 12 to 71, thus varying mean free path $l \sim 8.9$ to 3.6 cm. Earlier experiments [2] had shown that these disordered geometries are an excellent experimental realization of the classic problem of an electron in a 2D disordered potential. Subsequent to this work, there have been important theoretical developments [4,5,9], some motivated by our earlier experiments.

The experimental eigenfunctions directly demonstrate the trend toward decreasing localization from disordered to chaotic to integrable as seen in Fig. 1, which shows representative experimental eigenfunctions, along with their corresponding IPR I_2, for several billiards. The strongly localized state Fig. 1(a) at $f = 3.04$ GHz of the disordered billiard with $N = 36$ scatterers has very large $I_2 = 13.42$. Note that this is a direct observation of localization of EM waves which also maps to QM (matter) waves. In contrast the more delocalized state at higher frequency $f = 7.33$ GHz [Fig. 1(b)] explores almost all the available coordinate space similar to chaotic cavities and has a smaller $I_2 = 4.06$. For the chaotic Sinai stadium, typical values of the IPR are around 3.0 [$I_2 = 3.01$ for this eigenfunction Fig. 1(c)] while for the integrable rectangle billiard Fig. 1(d) IPR $I_2 = 2.25$ for all eigenfunctions. Figure 1 demonstrates a key advantage of our experiments, which is that by varying l and wave vector k we are able to access a wide range of the disorder strength kl, from strongly localized states for $kl < 1$ to delocalized states with $kl \gg 1$.

Eigenfunctions such as in Fig. 1 were then analyzed in terms of I_2 and $P_{I_2}(I_2)$. In the following, for convenience, we use the notation $I_2 = \int |\Psi(r)|^4 \, d\upsilon = \int u^2 \, d\upsilon$, $w = (I_2 - 3)/6$, $u = |\Psi(r)|^2$, and $I_1 = \int |\Psi(r)|^2 \, d\upsilon = 1$, and the integral is over the volume υ (area in 2D). Nearly 400 eigenfunctions were analyzed each containing more than 3200 eigenfunction values.

Figure 2 shows level-to-level variations $I_2(E)$ for the Sinai stadium. Here I_2 is mainly clustered around a mean value of $\langle I_2 \rangle = 3.0$, with relatively small level-to-level fluctuations. The IPR distribution $P_{I_2}(I_2)$ of the chaotic Sinai-stadium billiard is shown in Fig. 3 (top panel). $P_{I_2}(I_2)$ is seen to be a nearly symmetric distribution with a small width $I_2 - \langle I_2 \rangle \ll \langle I_2 \rangle$.

Reference [2] demonstrated that the Sinai-stadium billiard data obey the universal PT distribution $P_u(u) = (2\pi u)^{-1/2} \exp(-u/2)$, with $u = |\Psi|^2$ to a remarkable degree, while deviations from PT were demonstrated due to localization in the disordered billiards. The IPR for PT distribution can be immediately obtained $I_2 = \int_0^\infty u^2 P_u(u) \, du = 3.0$, which is a universal value. Note that there are no fluctuations expected about this universal value in RMT, i.e., $P_{I_2}(I_2)$ is a δ function at $I_2 = 3$ [10]. Clearly boundary scattering on the system length scale R leads to nonuniversal correlations (e.g., from periodic orbits leading to scars in the wave functions). This breaks the assumption in RMT of Gaussian fluctuations of the eigenfunction amplitude, and in turn leads to fluctuations

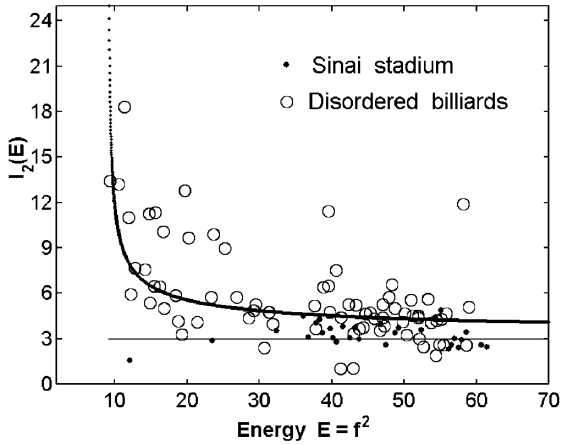

FIG. 2. Large level-to-level fluctuations are observed in the IPR $I_2(E)$ vs E of the disordered billiard ($l = 5.1$ cm). Also note the gradual trend towards a universal limiting value of 3.0 indicated by the solid line which represents a model described in the text. The fluctuations of the Sinai stadium are much smaller and are clustered around $\langle I_2 \rangle = 3.0$.

in the distribution $P_{I_2}(I_2)$ (although of narrow width) observed in Fig. 3 (top panel).

Even more strikingly, the IPRs of the disordered billiards shown in Fig. 2 display a remarkably large spectrum of level-to-level fluctuations (Fig. 2). For small f, when $\lambda > l$, strong localization leads to large values of I_2 in the disordered cavity, which can be as high as ~ 20. It is worth noting that the density distributions $P_u(u)$ of the eigenfunctions deviate strongly from the PT distribution and are consistent with the large IPR values. In this paper we have focused on the billiards with $l = 8.9$ and $l = 5.1$ cm.

As f is increased (or λ is decreased), the IPR progressively decreases, approaching the universal limiting value

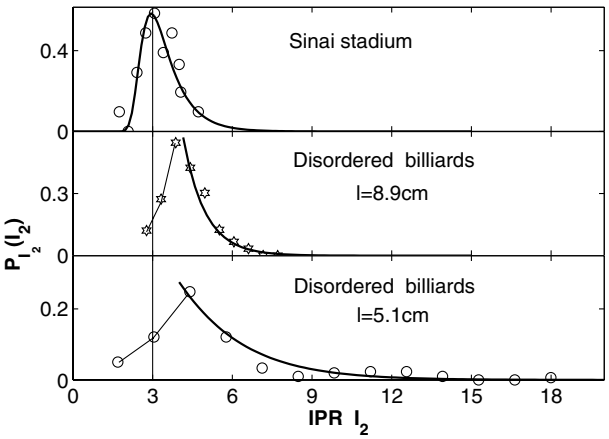

FIG. 3. IPR distributions $P_{I_2}(I_2)$ of the disordered billiards with $l = 8.9$ cm (middle panel) and $l = 5.1$ cm (bottom panel) are strongly asymmetric and non-Gaussian. The distribution for the chaotic Sinai-stadium billiard (top panel) is nearly symmetric about the mean value 3.0. The lines represent calculations based on the nonlinear sigma model.

of 3, as shown in Fig. 2. The corresponding distribution $P_{I_2}(I_2)$ shown in Fig. 3 (bottom) is strikingly different from the Sinai-stadium case, in that, it is strongly asymmetric, reflecting the very large $I_2 \gg \langle I_2 \rangle$ values that are present, and is strongly non-Gaussian. The IPR fluctuations in Fig. 2 are closely similar to the famous universal conductance fluctuations of a mesoscopic system.

Recently several theoretical studies have calculated the IPR distribution based on the supersymmetry method [4,5]. For a mesoscopic system the IPR distribution depends on the conductivity g of the system, defined as $g = \ln(R/l)/\langle w \rangle$, where R is the system size, l is the mean free path, and $\langle \cdots \rangle$ is the realization average for a fixed "disorder strength" $2kl$. The resulting probability distribution $P(I_2)$ for $I_2 < \langle I_2 \rangle = 3$ is [4]

$$P_{I_2}(I_2) = C_1 \frac{g}{2} \exp\Big[-\frac{g}{6}(I_2 - \langle I_2 \rangle) - \frac{\pi}{2} e^{-g/3[I_2 - \langle I_2 \rangle]}\Big], \quad (1)$$

and the corresponding distribution for $I_2 \gg \langle I_2 \rangle$,

$$P_{I_2}(I_2) = C_2 \sqrt{\frac{g}{I_2}} \exp\Big(-\frac{\pi}{6} g I_2\Big), \quad (2)$$

where C_1 and C_2 are normalization constants.

The solid lines in Fig. 3 (middle and bottom panels) represent Eq. (2) for $I_2 > \langle I_2 \rangle$ using conductivity values (middle panel) $g = 2.1$ for $l = 8.9$ cm and (bottom panel) $g = 1.0$ for $l = 5.1$ cm, and are seen to describe the data very well. Another way of presenting the comparison with Eq. (2) is by using a scaled variable $q = gI_2$ whence the distribution changes to a Porter-Thomas distribution in q. The system is within the weak disorder limit, i.e., the random phase approximation is still valid, and g depends weakly on the disorder factor $2kl$ [11]. Now rescaling the I_2 with g we obtain the distribution $P_q(q)$ (unnormalized) and plot $\ln[P_q(q)\sqrt{q}]$ vs q in Fig. 4. Both [correspond to Fig. 3 (middle and bottom panels)] show a straight line slope $= -1$ which implies a good agreement of theory and experiment for IPR distribution in a moderate disordered region where $I_2 \gg \langle I_2 \rangle$. This is the first experimental observation of the asymmetric distribution predicted by Prigodin and Altshuler [4].

We now return to the case of the Sinai stadium. Although a formulation in terms of a ballistic sigma model has been presented for chaotic cavities [12], it is not simply amenable to experimental comparison. Instead we use Eq. (1) with the assumption that since $l \approx R$, a suitably large conductivity ($g \gg 1$) can be used. In our experimental case, $g \approx 7.8$ matches Eq. (1) not only for $I_2 < \langle I_2 \rangle$, but also for $I_2 > \langle I_2 \rangle$, as shown in Fig. 3 (top panel). The nearly symmetric distribution can be understood since the fluctuations arise from correlations at the scale of the system length R, which is the only length scale in the problem. The values of g corresponding to the disordered billiards and the Sinai-stadium billiard are consistent with the $\langle w \rangle$ values and the mean free paths.

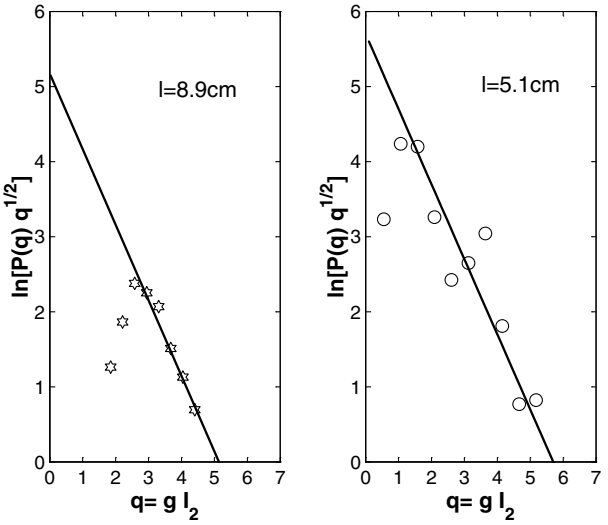

FIG. 4. The IPR distribution of Fig. 3 for the disordered billiards replotted (asymptotic part) using the scaled variable $q = gI_2$. Each solid line is the Porter-Thomas distribution vs q and agrees for large $I_2 \gg \langle I_2 \rangle$.

We now show that the experimental data also directly demonstrate the decay of spatial correlations $\langle \Psi^2(r)\Psi^2(r') \rangle$ of the eigenfunctions and obtain the decay length, which corresponds to the classical mean free path. To calculate the correlation with arbitrary disorder strength $2kl$, defining $K(r) = |\mathrm{Im}G(r')|^2/(\pi\nu)^2$, where $G(|r - r'|) = \langle r|(E - H)^{-1}|r' \rangle$ is the Green function of the disordered system Hamiltonian, then it can be shown [13] that $K(r) = |\frac{1}{\pi}\int_{-\infty}^{\infty} \frac{1}{1+y^2} J_0[kr(1 + \frac{1}{2kl}y)]\,dy|^2$.

For the chaotic or ballistic limit ($2kl \gg 1$), the result for Gaussian fluctuations is $\langle \Psi^2(r)\Psi^2(r') \rangle \simeq 1 + (I_2 - 1)J_0^2(r - r')$, where J_0 is the first order Bessel function. The correlation for a moderate disordered case with correct limits can be derived repeating the calculations of Ref. [14]

$$\langle \Psi^2(r)\Psi^2(r') \rangle \simeq 1 + (I_2 - 1)K(k|r - r'|) \quad (3)$$

$$\simeq 1 + (I_2 - 1)J_0^2(k|r - r'|)e^{-k|r-r'|/kl}. \quad (4)$$

These are valid when $r - r' \lesssim l$. We have solved $K(k|r - r'|)$ numerically. In Fig. 5, we plot the average correlation derived from experimental data, numerical calculations of Eq. (3), and analytical expression of Eq. (4) for different disorder strengths $2kl$. For the Sinai billiards, the average correlation starts at 3 and tends to 1 via Friedel oscillations, consistent with Eq. (4) with $2kl = 37$, which is very large and hence the result is close to that of the universal dependence given by $kl = \infty$. For disordered billiards, the autocorrelation is very large ($\sim I_2$) for short lengths, i.e., around $|r - r'| \approx 0$ due to localization, but the autocorrelation decays with a decay length scale, responsible for fast fall, and it should go to zero at large

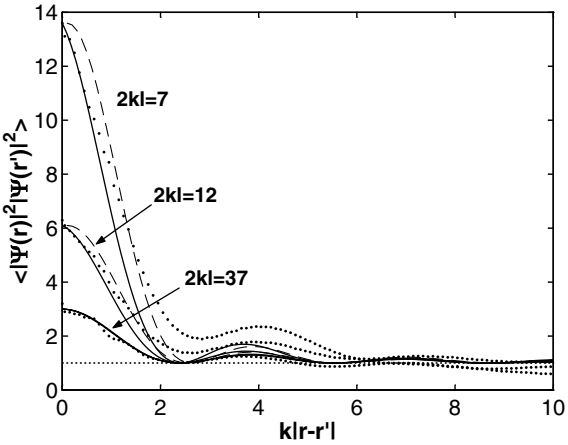

FIG. 5. Density autocorrelation $\langle \Psi^2(r)\Psi^2(r')\rangle$ of eigenfunctions of the Sinai stadium and disordered billiards with fixed disordered strength $2kl$. Experiment (dotted lines), Eq. (3) (dashed lines), and Eq. (4) with $2kl = 7$, 12, and 37 (solid lines).

$k|r - r'|$. The experimental data show good agreement with the numerical and analytical calculations for moderate disorder, as shown in Fig. 5 for values $2kl = 12$ and 7. These values are in excellent agreement with the corresponding mean free paths ($l = 3.6$, 5.1, 5.9, and 8.9 cm) obtained by directly considering the number of scatterers N, so that $l \sim \sqrt{ab/N}$, and a and b are the sides of the enclosing rectangle. Thus our analysis directly demonstrates localization and yields a quantitative measure in terms of the correlation decay length.

Returning to the level-to-level I_2 data in Fig. 2 we note that they can be viewed as tuning the degree of localization by varying energy E. Representing the IPR as $I_2(E) = I_{2,\mathrm{sm}}(E) + \delta I_2(E)$, i.e., a smooth part $I_{2,\mathrm{sm}}(E)$ plus fluctuations $\delta I_2(E)$, we discuss the trends in $I_2(E)$. Calculations in Ref. [15] based on the infinite dimensional tight binding model show that $I_2(E)$ diverges exponentially near the critical point E_c: $I_2(E) = I_2(E = \infty) \times \exp(A/|E - E_c|^{\mu})$, with $\mu = \frac{1}{2}$, due to very strong correlations of the wave function near E_c. $I_2(E = \infty)$ will be obviously the asymptotic universal value 3 as predicted by RMT in 2D. Our experimental IPR data are as large as IPR $\sim$ 20 (strongly localized), decaying to $\sim$4 (weakly localized) at high frequencies up to 10 GHz. In the present case, the smallest scale of the system $\sim$5 cm sets a natural lower cutoff frequency $f_c = c/2l = 3$ GHz, so that there are no eigenstates for $E < E_c = f_c^2$. For $E \gg E_c$ expanding the above equation in first order, we obtain $I_{2,\mathrm{sm}}(E) \simeq 3 + B/|E - E_c|^{\mu}$. In Fig. 2 we have plotted this expression with $\mu = 0.5$ and $B = 9.0$ (obtained by a best fit) and compared with the experimental data. The above expression captures the trend of the data. While an exact comparison with any expression is difficult since the fluctuations $\delta I_2(E) > I_{2,\mathrm{sm}}(E)$, the analysis illustrates that we are observing a frequency driven path from strong to weak localization in a disordered medium in terms of the IPR.

We have shown that the IPR is an extremely valuable parameter to study real-space localization in quantum eigenfunctions. We have demonstrated for the first time a quantitative analysis of features well beyond universality due to localization in experimental eigenfunctions. The observed IPR distribution is strongly non-Gaussian due to the correlations induced by scattering. The nonlinear sigma model is in quantitative agreement with the experimental data for moderate localization. Our work thus provides experimental support for the approach based upon quantum diffusion in the localization regime.

This work was supported by NSF-PHY-9722681. We thank A. Kudrolli for useful discussions. S. S. is grateful for the hospitality of the Quantum Chaos Workshop at the Australian National University, Canberra, where part of this work was carried out.

[1] M. C. Gutzwiller, *Chaos in Classical and Quantum Mechanics* (Springer, New York, 1990).
[2] A. Kudrolli, V. Kidambi, and S. Sridhar, Phys. Rev. Lett. **75**, 822 (1995).
[3] K. B. Efetov, *Supersymmetry in Disorder and Chaos* (Cambridge University, Cambridge, England, 1997).
[4] V. N. Prigodin and B. L. Altshuler, Phys. Rev. Lett. **80**, 1944 (1998).
[5] A. D. Mirlin, cond-mat/9907126 [Phys. Rep. (to be published)].
[6] (a) S. Sridhar, Phys. Rev. Lett. **67**, 785 (1991); (b) S. Sridhar, D. Hogenboom, and B. A. Willemsen, J. Stat. Phys. **68**, 239 (1992).
[7] (a) M. Barth, U. Kuhl, and H.-J. Stöckmann, Phys. Rev. Lett. **82**, 2026 (1999); (b) H. Alt *et al.,* Phys. Rev. Lett. **74**, 62 (1995); (c) L. Sirko, P. Koch, and R. Blumel, Phys. Rev. Lett. **78**, 2940 (1997).
[8] W. Lu, M. Rose, K. Pance, and S. Sridhar, Phys. Rev. Lett. **82**, 5233 (1999).
[9] V. I. Fal'ko and K. B. Efetov, Phys. Rev. B **50**, 11 267 (1994).
[10] M. Srednicki, Phys. Rev. E **54**, 954 (1996).
[11] P. Pradhan, e-print cond-mat/9703255.
[12] B. A. Muzykantskii and D. E. Khmelnitskii, Phys. Rev. E **51**, 5480 (1995).
[13] V. N. Prigodin, B. L. Altshuler, K. B. Efetov, and S. Iida, Phys. Rev. Lett. **72**, 546 (1994).
[14] V. N. Prigodin, N. Taniguchi, A. Kudrolli, V. Kidambi, and S. Sridhar, Phys. Rev. Lett. **75**, 2392 (1995).
[15] Y. V. Fyodorov and A. D. Mirlin, Phys. Rev. B **55**, 16 001 (1997).